ORGANOMETALLICS
Article

Organometallics **2011,** *30,* 263–272 263
DOI: 10.1021/om100897j

Chiral-at-*ansa*-Bridged Group 4 Metallocene Complexes {(R^1R^2C)-(3,6-tBu$_2$Flu)(3-R^3-5-Me-C_5H_2)}MCl_2: Synthesis, Structure, Stereochemistry, and Use in Highly Isoselective Propylene Polymerization

Evgeny Kirillov,*[,†,‡] Nicolas Marquet,[†] Manuela Bader,[†] Abbas Razavi,[§] Vincenzo Belia,[§] Frank Hampel,[‡] Thierry Roisnel,[†] John A. Gladysz,*[,‡,⊥] and Jean-François Carpentier*[,†]

[†]*Organometalliques et Catalyse, UMR 6226 CNRS-Université de Rennes 1, 35042 Rennes Cedex, France,* [‡]*Institut für Organische Chemie, Friedrich-Alexander Universität Erlangen-Nürnberg, Henkestrasse 42, 91054 Erlangen, Germany,* [§]*Total Petrochemicals, Zone Industrielle C, 7181 Feluy, Belgium, and* [⊥]*Department of Chemistry, Texas A&M University, P.O. Box 30012, College Station, Texas 77842-3012, United States*

Received September 17, 2010

New chiral racemic, sterically crowded fluorenyl-cyclopentadienyl compounds having monoaryl-substituted methylene bridges (R^1R^2C)-((3,6-tBu$_2$Flu)H)(3-R^3-5-Me-C_5H_3) (R^1 = H, R^2 = Ph, R^3 = tBu: **2a**; R^1 = H, R^2 = 2,4,6-$Me_3C_6H_2$ (Mes); R^3 = CMe_2Ph (cumyl): **2b**; R^1 = H, R^2 = 3,5-$(CF_3)_2C_6H_3$, R^3 = tBu: **2c**) or a disubstituted (R^1 = CF_3, R^2 = Ph, R^3 = tBu: **2d**) as well as an unsubstituted (nonstereogenic) methylene bridge (R^1 = R^2 = H, R^3 = tBu: **2e**) were synthesized via nucleophilic additions to substituted fulvenes. The zirconium and hafnium dichloro complexes derived from proligands **2a**, **2b**, and **2e**, namely, {Ph(H)C-(3,6-tBu$_2$Flu)(3-tBu-5-Me-C_5H_2)}$ZrCl_2$ (**3a**), {Ph(H)C-(3,6-tBu$_2$Flu)(3-tBu-5-Me-C_5H_2)}-$HfCl_2$ (**4a**), {Mes(H)C-(3,6-tBu$_2$Flu)(3-cumyl-5-Me-C_5H_2)}$ZrCl_2$ (**3b**), and {H_2C-(3,6-tBu$_2$-Flu)(3-tBu-5-Me-C_5H_2)}$ZrCl_2$ (**3e**), were prepared (63−88% yields). Attempted metalations at the fluorinated proligands **2c** and **2d** were not successful. Due to the presence of the stereogenic center of the *ansa*-bridge, **3a**, **4a**, and **3b** exist as mixtures of two diastereomers in which the most bulky substituent in the methylene bridge is either *anti* (major product in the case of **3a** and **4a**) or *syn* (only one observed for **3b**) to the 5-methyl substituent in the Cp ring. Diastereomerically pure ***anti*-3a**, ***anti*-4a** and ***syn*-4a**, and ***syn*-3b** were isolated and characterized by elemental analysis, NMR spectroscopy, and X-ray crystallography. When activated with MAO, metallocene complex ***anti*-3a** showed very high activity in the polymerization of propylene (14 000 kg(PP)·mol(Zr)$^{-1}$·h^{-1}, toluene, 60 °C) to yield highly isotactic polypropylene (iPP) with $[m]^4$ = 95.8% and T_m = 153 °C. Both diastereomers of hafnium analogues exhibited lower activities (260−270 kg(PP) mol(Hf)$^{-1}$·h^{-1}) but distinct catalytic behavior: ***anti*-4a** yielded low molecular weight and moderately isotactic PP ($[m]^4$ = 88.8%), while highly isotactic PP ($[m]^4$ = 94.0%) with a bimodal distribution was produced with ***syn*-4a**. Precursor ***syn*-3b** was inactive under standard polymerization conditions, presumably due to deactivation of the cationic metal center by the cumyl Cp substituent. Methylene-bridged **3e** produced highly isotactic PP ($[m]^4$ = 96.9%; T_m = 154 °C) with moderate activity (2 320 kg(PP)·mol(Zr)$^{-1}$·h^{-1}).

Introduction

Carbon-linked mixed fluorenyl-cyclopentadienyl ligands (hereafter referred to as {Flu-Cp}$^{2-}$) are of significant importance in the academic and industrial communities because of the remarkably high catalytic activity and stereoselectivity that some group 4 metal complexes derived therefrom feature in olefin polymerization.[1,2] In a previous study, we have investigated the preparation of new C_1-symmetric *ansa*-zirconocene complexes bearing diaryl-substituted methylene-bridged {R^1R^2C-(Flu)(Cp)}$^{2-}$ ligands (**I-R^1R^2**, Scheme 1) that produce isotactic polypropylene via an enantiomorphic-site control mechanism.[3] Special emphasis was given to the Ph_2C-bridged system (**I-Ph_2**), which was anticipated to provide improved catalytic performances but remained elusive for years due to synthetic challenges. In fact, the latter compound could be effectively prepared via an "activated fulvene" pathway and was shown to afford enhanced catalytic

*Corresponding authors. E-mail: evgueni.kirillov@univ-rennes1.fr, gladysz@mail.chem.tamu.edu, jean-francois.carpentier@univ-rennes1.fr.

(1) For leading references, see: (a) Ewen, J. A.; Jones, R. L.; Razavi, A. *J. Am. Chem. Soc.* **1988**, *110*, 6255. (b) Razavi, A.; Bellia, V.; De Brauwer, Y.; Hortmann, K.; Peters, L.; Sirol, S.; Van Belle, S.; Thewalt, U. *Macromol. Chem. Phys.* **2004**, *205*, 347.

(2) For reviews, see: (a) Alt, H.; Samuel, E. *Chem. Soc. Rev.* **1998**, 323. (b) Alt, H. *Macromol. Chem. Symp.* **2001**, *173*, 65. (c) Razavi, A. *Coord. Chem. Rev.* **2006**, *250*, 155. (d) Alt, H. G.; Köppl, A. *Chem. Rev.* **2000**, *100*, 1205. (e) Coates, G. W. *Chem. Rev.* **2000**, *100*, 1223. (f) Resconi, L.; Cavallo, L.; Falt, A.; Piemontesi, F. *Chem. Rev.* **2000**, *100*, 1253. (g) Gladysz, J. A. Special issue: Frontiers in Metal-Catalyzed Polymerization. *Chem. Rev.* **2000**, *100*, 1167. (h) Price, C. J.; Irwin, L. J.; Aubry, D. A.; Miller, S. A. Fluorenyl Containing Catalysts for Stereoselective Propylene Polymerization. In *Stereoselective Polymerization with Single Site Catalysts*; Baugh, L. S.; Canich, J. A. M., Eds.; CRC Press, 2000.

(3) Kirillov, E.; Marquet, N.; Razavi, A.; Belia, V.; Hampel, F.; Roisnel, T.; Gladysz, J. A.; Carpentier, J.-F. *Organometallics* **2010**, *29*, 5073.

Published on Web 12/22/2010

Scheme 1

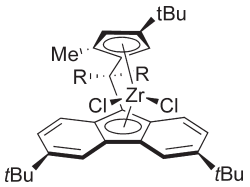

I-Me$_2$ (R = Me)
I-Ph$_2$ (R = Ph)

Scheme 2

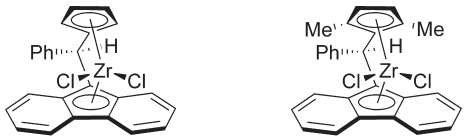

II III

activity (2−3-fold increase as compared to the corresponding isopropylidene-bridged system **I-Me$_2$**) for the highly isoselective polymerization of propylene under homogeneous conditions.[3] Yet, the complicated and relatively costly synthetic approach required for preparing **I-Ph$_2$** prompted us to seek other more synthetically attainable *ansa*-metallocene systems {R^{1}R^{2}C-(Flu)(Cp)}MCl$_2$ that contain phenyl substituent(s) in the ligand methylene bridge.

Our attention was directed toward ligand assemblies (and corresponding metallocene complexes) having a single aryl substituent at the methylene bridge. Syndioselective zirconocene systems with a Ph(H)C bridge in the C_s-symmetric {R^{1}R^{2}C-(Flu)(Cp)} ligand skeleton (Scheme 2) were first reported by Alt (**II**)[4] and subsequently developed by Lee et al. (**III**).[5] However, similar isoselective systems with a Ph(H)C bridge in C_1-symmetric ligand skeletons remain undocumented to the best of our knowledge.[2]

We report herein new C_1-symmetric group 4 metallocene complexes supported by {R^{1}R^{2}C-(Flu)(Cp)}$^{2-}$ ligands that incorporate monoaryl-substituted or unsubstituted methylene bridges. The central objective of this investigation was to assess the impact of such bridges on the catalytic performances for the production of isotactic polypropylene; in particular, it was of interest to evaluate (i) the effect of a single aryl substituent upon reactivity, in comparison with diaryl-substituted systems, and (ii) the influence of the stereogenic center present in the bridge that induces the formation of two diastereomeric *ansa*-metallocene species, which may have distinct catalytic behaviors. Thus, the title complexes have, after activation by MAO, been investigated as homogeneous catalysts for the polymerization of propylene. Their performances are compared to those of the prototype precatalyst {Me$_2$C-(3,6-*t*Bu$_2$Flu)(3-*t*Bu-5-MeC$_5$H$_2$)}ZrCl$_2$ (**I-Me$_2$**) and its more sterically encumbered variant {Ph$_2$C-(3,6-*t*Bu$_2$Flu)-(3-*t*Bu-5-MeC$_5$H$_2$)}ZrCl$_2$ (**I-Ph$_2$**), which we have recently investigated.[3]

Results and Discussion

Synthesis of Proligands. Nucleophilic additions of fluorenyl-type anions to fulvenes have been shown to provide the most versatile and efficient routes for the synthesis of the monocarbon-bridged proligands {R^{1}R^{2}C-(Flu)(Cp)}H$_2$.[6] Accordingly, a series of fulvene building blocks **1a**−**e** were prepared by the well-established pathway in Scheme 3. In a previous study, we have investigated the synthesis of sterically hindered diphenylmethylene-bridged proligands via this route.[3,7] However, the direct approach, involving reaction between a fluorenyl anion and 6,6′-diphenylfulvenes, appeared to be inoperative for Ph$_2$C-bridged systems having a 5-methyl substituent in the cyclopentadienyl ring, due to steric and electronic reasons. In this study, we have found that the somewhat less congested 6-monoarene fulvenes **1a** and **1d** can be treated with {3,6-*t*Bu$_2$Flu}$^-$Li$^+$ under mild conditions (THF, room temperature; Scheme 3, protocol C) to afford the corresponding adducts in satisfactory yields (49−65%).[8] The mesityl-substituted derivative **1b** could be induced to condense only in diethyl ether at 90 °C (in an autoclave) over several days (Scheme 3, protocol D), although a satisfactory yield was attained under these conditions.[9] This striking difference in efficiency obviously arises from the presence of an *ortho*-methyl-substituted aryl ring, which increases steric hindrance in the fulvene, as compared to simple phenyl (**1a**, **1d**). On the other hand, proligand **2c**, derived from *meta*-bis(trifluoromethyl)aryl-substituted fulvene (**1c**), could be obtained only in very small amounts (isolated yield: 4%; protocol C).[10] For comparison purposes, the unsubstituted methylene-bridged proligand **2e** was prepared in 60% yield using the procedure disclosed by Alt et al.,[11] via the reaction of 6-dimethylaminofulvene **1e** with {3,6-*t*Bu$_2$Flu}$^-$Li$^+$ in THF solution at room temperature, followed by treatment with LiAlH$_4$. Proligands **2a**−**e** were isolated as air-stable crystalline solids, and their identities were authenticated by NMR spectroscopy and elemental analysis.

Synthesis and Structure of *ansa*-Metallocene Complexes. Zirconium and hafnium *ansa*-metallocene complexes were obtained from the corresponding tetrachlorides MCl$_4$ and ligand dianions, prepared *in situ* via addition of 2 equiv of *n*-butyllithium, using a regular salt metathesis protocol in diethyl ether (see the Experimental Section). Analytically pure zirconium complexes **3a**, **3b**, and **3e** (pink crystalline solids) and hafnium complex **4a** (yellow-orange crystalline solid) were thus isolated in good yields (Scheme 4). On the other hand, all attempts to prepare *ansa*-metallocene complexes based on fluorinated proligands **2c** and **2d** led to mixtures of compounds that could not be purified.

(4) Alt, H. G.; Zenk, R. *J. Organomet. Chem.* **1996**, *518*, 7.
(5) Won, Y. C.; Kwon, H. Y.; Lee, B. Y.; Park, Y.-W. *J. Organomet. Chem.* **2003**, *677*, 133.

(6) For relevant procedures, see: (a) Day, J. H. *Chem. Rev.* **1953**, *53*, 167. (b) Alt, H.; Jung, M. *J. Organomet. Chem.* **1998**, *568*, 87. (c) Alt, H. G.; Jung, M.; Kehr, J. *J. Organomet. Chem.* **1998**, *562*, 153. (d) Miller, S. A.; Bercaw, J. E. *Organometallics* **2002**, *21*, 934. (e) Miller, S. A.; Bercaw, J. E. *Organometallics* **2004**, *23*, 1777.
(7) Carpentier, J.-F.; Kirillov, E.; Razavi, A. (Université de Rennes 1 and Total Petrochemicals Co.) *Eur. Pat. Appl.* EP06121181.9,Sept 25, 2006.
(8) (a) Kirillov, E.; Gladysz, J. A.; Razavi, A. (Friedrich-Alexander Universität Erlangen-Nürnberg and Atofina Co.) *Eur. Pat. Appl.* EP05105162.1, June 13, 2005.
(9) Solvent effects in the nucleophilic addition of the fluorenyl anion to sterically protected fulvenes have been noticed in our previous study; see ref 3.
(10) The small amount of proligand **2c** isolated was sufficient to explore its metalation and coordination onto Zr, which eventually turned out unsuccessful (*vide infra*). Optimization of the synthesis of this compound, e.g., using protocol D, was therefore not further investigated.
(11) (a) Zenk, R.; Alt, H. G.; Welch, B. M.; Palackal, S. J. (Philips Petroleum Co.) U.S. Patent 5420320, 1995. (b) Alt, H. G.; Zenk, R. *J. Organomet. Chem.* **1996**, *526*, 295.

Scheme 3. Synthesis of Fulvenes 1a−e and $\{R^1R^2C\text{-}(Flu)(Cp)\}H_2$ Proligands 2a−e

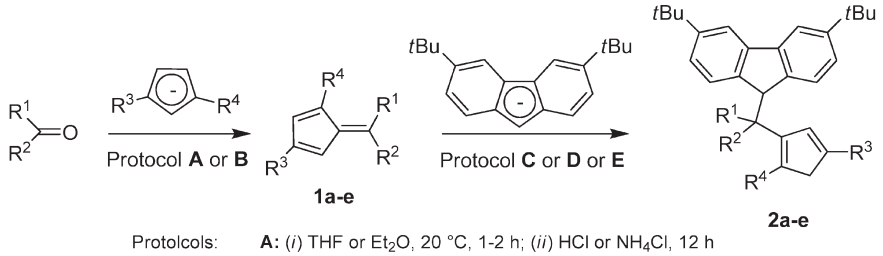

Protolcols: **A:** (*i*) THF or Et_2O, 20 °C, 1-2 h; (*ii*) HCl or NH_4Cl, 12 h
B: (*i*) instead of ketone, $(MeO)_2SO_2$/DMF was used
C: (*i*) THF, 20 °C, 4 h; (*ii*) H_3O^+
D: (*i*) Et_2O, 90 °C, 50-70 h; (*ii*) H_3O^+
E: (*i*) THF, 20 °C, 12 h; (*ii*) $LiAlH_4$, reflux, 12 h; (*iii*) H_3O^+

R_1	R_2	R_3	R_4	Fulvene	Proc.	Yield (%)	Proligand	Proc.	Yield (%)
H	Ph	*t*Bu	Me	**1a**	**A**	31	**2a**	**C**	65
H	2,4,6-$Me_3C_6H_2$	CMe_2Ph	Me	**1b**	**A**	66	**2b**	**D**	67
H	(3,5-CF_3)$_2C_6H_3$	*t*Bu	Me	**1c**	**A**	35	**2c**	**C**	4
CF_3	Ph	*t*Bu	Me	**1d**	**A**	25	**2d**	**C**	49
H	NMe_2	*t*Bu	Me	**1e**	**B**	23	**2e**[a]	**E**	60

[a] $R^1 = R^2 = H$; the NMe_2 group is replaced by hydride during the $LiAlH_4$ step in protocol **E**

Scheme 4. Syntheses and Isolated Yields of Group 4 *ansa*-Metallocene Complexes Derived from Proligands 2a, 2b, and 2e[a]

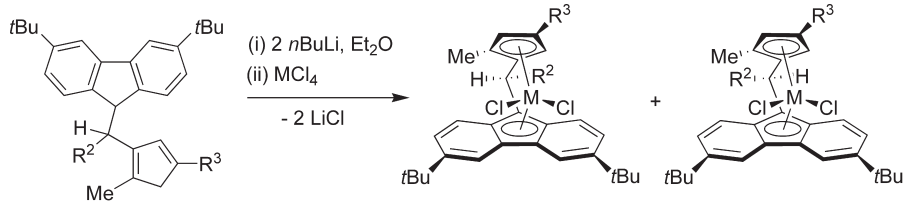

2a (R^2 = Ph, R^3 = *t*Bu)
2b (R^2 = 2,4,6-$Me_3C_6H_2$, R^3 = CMe_2Ph)
2e (R^2 = H, R^3 = *t*Bu)

R^2 = Ph, R^3 = *t*Bu:
M = Zr
***anti*-3a** (40%) ***syn*-3a** (not isolated)
M = Hf
***anti*-4a** (55%) ***syn*-4a** (18%)

R^2 = 2,4,6-$Me_3C_6H_2$, R^3 = CMe_2Ph:
M = Zr
***anti*-3b** (not observed) ***syn*-3b** (63%)

R^2 = H, R^3 = *t*Bu:
M = Zr
3e (64%)

[a] Only one enantiomer is shown for each diastereomer.

Since **3a**, **3b**, **3e**, and **4a** were derived from racemic proligands, they were presumed to be racemates. Their solution structures were investigated by ^1H and ^{13}C NMR spectroscopy. The NMR spectra of racemic **3e**, the only complex with an unsubstituted methylene bridge, featured only one set of resonances, consistent with the presence of a single C_1-symmetric species in solution. On the other hand, due to the existence of an additional element of chirality, i.e., the stereogenic center in the substituted methylene bridge of **3a**, **4a**, and **3b**, two diastereomers for each of these compounds were anticipated (Scheme 4). This was corroborated by ^1H NMR spectra of crude (nonrecrystallized) complexes, for which two sets of resonances for unequal amounts of two diastereomers were generally observed. Thus, the crude zirconium complex **3a** appeared to be a ca. 90:10 mixture of two diastereomers. The predominant isomer would logically be that in which the phenyl substituent in the methylene bridge is positioned *anti* to the methyl group in the Cp ring (***anti*-3a**, as further corroborated by X-ray analysis, *vide infra*). Minimization of steric repulsion between these substituents is likely at the origin of the faster formation and/or greater thermodynamic stability of the latter isomer, as opposed to the *syn* isomer (***syn*-3a**), in which the methyl and phenyl groups are obviously much closer (*vide infra*). Also, crude

hafnium compound **4a** was recovered in a quite different (as compared to its zirconium congener, **3a**) diastereomeric ratio (***anti*-4a**/***syn*-4a** = 70:30), despite the similar size of these metal centers (ionic radius for six-coordinate metal centers, Hf^{4+}: 0.71 Å vs Zr^{4+}: 0.72 Å).[12] This indicates that the diastereomeric ratio in this metalation reaction is apparently affected by the stereoelectronic environment of the metal (precursor), but not by its ionic radius.

In contrast, for complex **3b**, only one diastereomer was detected by NMR spectroscopy. Further crystallographic investigations (*vide infra*) revealed it is that in which the bulky mesityl substituent in the methylene bridge is directed to the same side as the methyl substituent in the Cp ring, that is, *cis*-Me,Mes (***syn*-3b**). There is no obvious explanation that would rationalize the selective formation of this diastereomer on steric grounds. Rather, this could imply that this is a kinetically controlled process.

In addition to confirming the formation of these diastereomers, ^{13}C NMR spectroscopy revealed particularly upfield chemical shifts for the C9-fluorenyl carbon (δ 70.3−76.6 ppm). These data suggest reduced hapticity ($\eta^5 \rightarrow \eta^3$ ring slippage) of the fluorenyl moiety in solution.[13] Otherwise, the ^{13}C NMR data do not indicate significant differences in solution structures in this series of *ansa*-metallocene complexes.

The pure diastereomer ***anti*-3a** was isolated in good yield by recrystallization of the 90:10 *anti*/*syn* crude material. With **4a**, the less biased diastereomeric ratio (70:30) allowed successful isolation of both ***anti*-4a** and ***syn*-4a**, also by recrystallization. Single crystals of ***anti*-3a**, ***syn*-3b**, **3e**, ***anti*-4a**, and ***syn*-4a** suitable for X-ray diffraction studies were prepared from concentrated solutions in dichloromethane/hexane mixtures or neat hexane at room temperature. The molecular structures of these metallocene compounds are depicted in Figures 1−5, and selected crystallographic and geometrical parameters are given in Tables 1 and 2, respectively. The elementary units of the C_1-symmetric complex **3e** and diastereomerically pure ***anti*-3a**, ***syn*-3b**, ***anti*-4a**, and ***syn*-4a** are all composed of pairs of enantiomers. That of ***syn*-4a** contains two independent molecules.

These compounds feature geometrical parameters similar to those documented for other metallocene dichlorides incorporating Me_2C-, Ph_2C-, and Ph(H)C-bridged {R^1R^2C-(Flu)-(Cp)} ligands.[5,14] In agreement with our previous observations on {Ph_2C-(3,6*t*Bu_2Flu)(Cp)}MCl_2 complexes,[3] all the new *ansa*-metallocene complexes reported herein display a slight deviation of the η^5-coordination of the fluorenyl central five-membered ring to the metal atom toward a reduced η^3-mode, as evidenced by the significant differences in the M−C(ring) distances. In line with the close ionic radii of Zr and Hf metals, the $Cp_{cent}-M-Flu_{cent}$ bite angles in ***anti*-3a** and ***anti*-4a** are quite similar (118.1(1)° and 118.7(3)°, respectively). Note that the latter compounds are isostructural. The bite angle in ***syn*-4a** is modestly larger (119.6(2)°), possibly as a consequence of the steric repulsion between the bridge and Cp substituents. Also, a significant constraint at the bridging carbon atom in this *ansa*-metallocene complex is evidenced from the value of 98.7(2)° for the C(1)−C(6)−C(9) angle; the latter angle is ca. 3° tighter than those observed in its congeners. In contrast, the $Cp_{cent}-Zr(1)-Flu_{cent}$ bite angle in ***syn*-3b** is somewhat more constrained (116.7(2)°), that is,

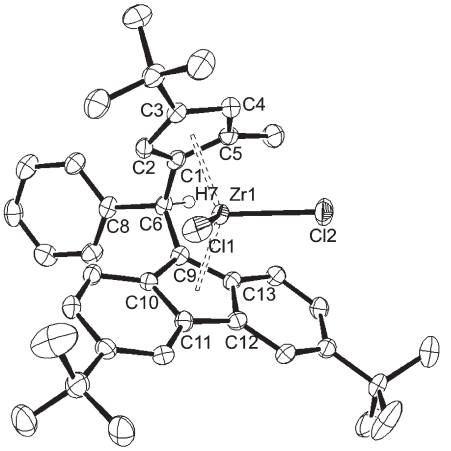

Figure 1. Crystal structure of *anti*-{Ph(H)C-(3,6-*t*Bu_2Flu)-(3-*t*Bu-5-Me-C_5H_2)}$ZrCl_2$ (***anti*-3a**) (ellipsoids drawn at the 50% probability level; all hydrogen atoms, except that of the bridge, are omitted for clarity; only one enantiomer is depicted).

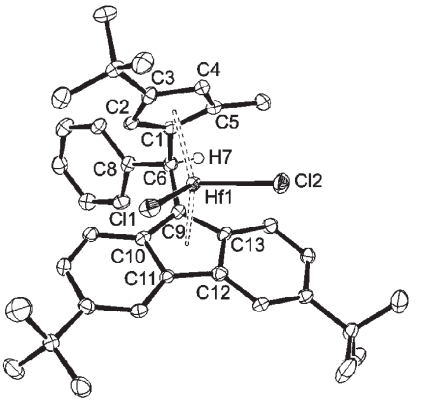

Figure 2. Crystal structure of *anti*-{Ph(H)C-(3,6-*t*Bu_2Flu)-(3-*t*Bu-5-Me-C_5H_2)}$HfCl_2$ (***anti*-4a**) (ellipsoids drawn at the 50% probability level; all hydrogen atoms, except that of the bridge, are omitted for clarity; only one enantiomer is depicted).

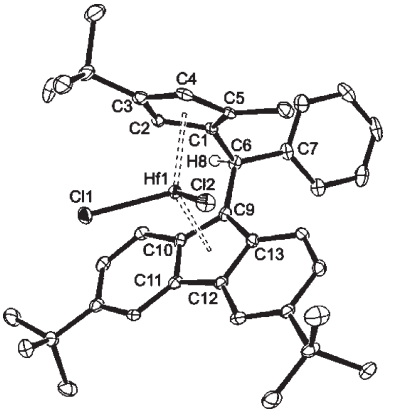

Figure 3. Crystal structure of one of the two independent molecules of crystalline *syn*-{Ph(H)C-(3,6-*t*Bu_2Flu)(3-*t*Bu-5-Me-C_5H_2)}$HfCl_2$ (***syn*-4a**) (ellipsoids drawn at the 50% probability level; all hydrogen atoms, except that of the bridge, are omitted for clarity; only one enantiomer is depicted).

(12) Shannon, R. D. *Acta Crystallogr.* **1976**, *A32*, 751.
(13) (a) Irwin, L. J.; Reibenspies, J. H.; Miller, S. A. *Polyhedron* **2005**, *24*, 1314. (b) Drago, D.; Pregosin, P. S.; Razavi, A. *Organometallics* **2000**, *19*, 1802.
(14) Razavi, A.; Thewalt, U. *J. Organomet. Chem.* **2001**, *621*, 267, and references therein.

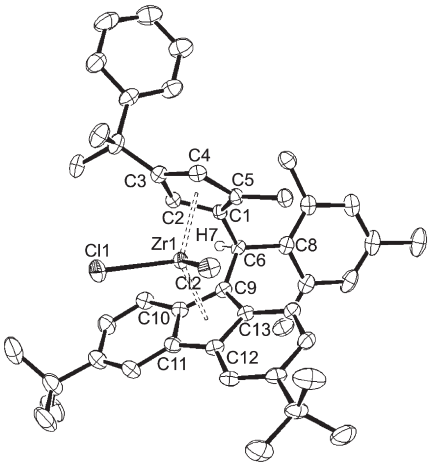

Figure 4. Crystal structure of *syn*-{Mes(H)C-(3,6-*t*Bu_2Flu)-(3-Cumyl-5-Me-C_5H_2)}$ZrCl_2$ (***syn*-3b**) (ellipsoids drawn at the 50% probability level; all hydrogen atoms, except that of the bridge, are omitted for clarity; only one enantiomer is depicted).

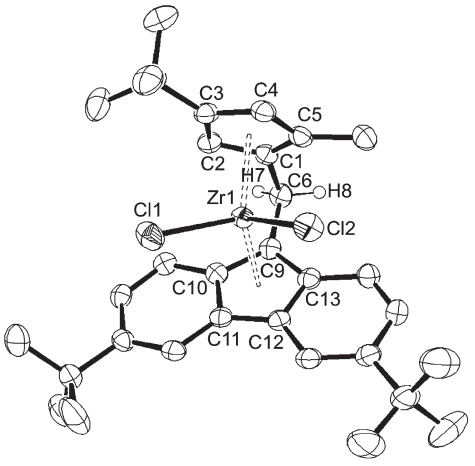

Figure 5. Crystal structure of {H_2C-(3,6-*t*Bu_2-Flu)(3-*t*Bu-5-Me-C_5H_2)}$ZrCl_2$ (**3e**) (ellipsoids drawn at the 50% probability level; all hydrogen atoms, except those of the bridge, are omitted for clarity; only one enantiomer is depicted).

ca. 2−3° smaller than those in the latter *ansa*-metallocene compounds.

Propylene Polymerization Catalysis. Diastereomerically pure *ansa*-metallocene complexes ***anti*-3a**, ***anti*-4a**, ***syn*-4a**, and ***syn*-3b**, as well as methylene-bridged **3e**, in combination with MAO, were evaluated in the homogeneous polymerization of propylene (toluene solutions, 5 bar constant pressure, T_{pol} = 40−60 °C).[15] For comparison purposes, the catalytic performances of the reference isopropylidene- and diphenylmethylene-bridged metallocene precatalysts **I-Me$_2$** and **I-Ph$_2$**[3] were determined under identical conditions. Selected polymerization results are summarized in Table 3.

Gratifyingly, the activity of the catalyst system based on ***anti*-3a** was found to be significantly higher than those of the reference systems **I-Me$_2$** and **I-Ph$_2$** (14 000 vs 1710 and 3580 kg PP·mol^{-1}·h^{-1} at 60 °C; compare entries 1, 2, and 4 in Table 3). This high activity generated significant exothermicity, so that reactions with ***anti*-3a**/MAO performed at an initial temperature of 40 °C (entry 3) rapidly rose to 55−60 °C. Polymerizations with this catalyst system were better conducted with low catalyst loadings (ca. 10 μmol) at a setting temperature of 60 °C (entries 4, 6); under such conditions, the exothermicity could be limited to 5−10 °C. On the other hand, the isotactic polypropylenes produced with **I-Me$_2$**, **I-Ph$_2$**, and ***anti*-3a** had similar characteristics. Replacement of the Me_2C or Ph_2C bridge for a Ph(H)C bridge did not induce significant changes in the molecular weight, molecular weight distribution, or stereoselectivity of the resultant polymer, as assessed by the GPC data, high pentad $[m]^4$ content, and T_m values (compare entries 1, 2, and 4). This was not unexpected in terms of stereoselectivity, because of the structural analogy of *ansa*-metallocene compounds **I-Me$_2$**, **I-Ph$_2$**, and ***anti*-3a** (and of the corresponding active species derived thereof). We also observed no major change either in activity or in properties of the polypropylenes produced when a 40:60 molar mixture of ***anti*-3a** and ***syn*-3a** diastereomers was used (entry 6).[16] This fact suggests that either the active species derived from both diastereomers of zirconocene complex **3a** have uniform catalytic properties or the activation of isomer ***syn*-3a** with MAO generates poorly active or completely inactive species. The latter hypothesis seems unlikely since the system ***anti*/*syn*-3a**/MAO behaved very similarly in terms of activity as the one composed of pure ***anti*-3a**.

Further raising the polymerization temperature to 80 °C did not improve the catalytic activity of the ***anti*-3a**/MAO system (entry 5), but rather resulted in a significant decrease of the molecular weight of polypropylene (at least by 3 times, attributable to enhanced β-H elimination) and stereoselectivity (from 95.8% down to 82.2% of isotactic pentads).

The activities of the systems based on hafnium analogues (***anti*-4a** and ***syn*-4a**) were found to be much lower, even when much larger catalyst loadings were used (activities up to 260 and 270 kg PP·mol^{-1}·h^{-1}, respectively, entries 7 and 8). The latter observation is in line with the almost complete inactivity in propylene polymerization recently reported for *ansa*-hafnocene complexes {R_2C-(Flu)(Cp)}$HfCl_2$ (R = Me, Ph) upon activation with commercial MAO.[17] Yet, interestingly enough despite the relatively low catalytic activities, the polypropylenes obtained independently with the two hafnium precatalysts featured quite different properties, as judged from their molecular weight distributions and microstructures. As compared to its structural *ansa*-zirconocene analogue (***anti*-3a**), precatalyst ***anti*-4a** gave lower molecular weight PP (72 vs 171 kDa) with significantly lower isotacticity ($[m]^4$ = 88.8 vs 94.8% and T_m = 142 vs 153 °C, respectively) (compare entries 7 and 4). At the same time, the ***syn*-4a**/MAO system yielded PP with a high isotactic content ($[m]^4$ = 94.0%), yet featuring a bimodal distribution, as evidenced by GPC and the observation of two endotherms

(15) Each polymerization experiment was independently repeated three times under the same conditions, revealing good reproducibility in terms of activity (gas uptake), productivity (polymer yield), and physicochemical properties (M_w, M_n, T_m, isotacticity) of the isolated polymer.

(16) This 40:60 molar diastereomeric mixture was obtained by evaporation/crystallization of the mother liquor obtained after the isolation of ***anti*-3a** diastereomer.

(17) The quite low polymerization activity of these hafnocene catalyst systems is a function of the remarkable propensity of cationic species of the type [{R_2C-(Flu)(Cp)}HfMe]$^+$ to form inactive "dormant" bimetallic species of the type [{R_2C-(Flu)(Cp)}Hf(μ-$Me)_2AlMe_2$]$^+$ through reaction with trimethylaluminium present in commercial MAO toluene solutions; see: Busico, V.; Cipullo, R.; Pellecchia, R.; Talarico, G.; Razavi, A. *Macromolecules* **2009**, *42*, 1789.

Table 1. Summary of Crystal and Refinement Data for *ansa*-Metallocene Complexes *anti*-3a, *anti*-4a, *syn*-4a, *syn*-3b, and 3e

	anti-3a	*anti*-4a	*syn*-4a	*syn*-3b	3e
empirical formula	$C_{38}H_{44}Cl_2Zr$	$C_{38}H_{44}Cl_2Hf$	$C_{76}H_{88}Cl_4Hf_2$	$C_{46}H_{52}Cl_2Zr$	$C_{32}H_{40}Cl_2Zr$
fw	662.85	750.12	1500.24	767.00	586.76
temp, K	173(2)	100(2)	100(2)	100(2)	173(2)
wavelength, Å	0.71073	0.71073	0.71073	0.71073	0.71073
cryst syst	monoclinic	monoclinic	triclinic	monoclinic	monoclinic
space group	$P2_1/c$	$P2_1/c$	$P\bar{1}$	$P2_1/n$	$P2_1/c$
a, Å	11.0734(2)	11.0044(8)	11.5420(10)	10.1294(4)	10.4377(2)
b, Å	26.3223(4)	26.201(2)	13.2190(10)	18.5232(9)	21.6825(6)
c, Å	11.6259(2)	11.5564(9)	22.043(3)	20.7106(9)	13.6979(3)
β, deg	101.831(1)	101.670(2)	97.850(10)	95.147(2)	106.509(1)
volume, Å^3	3316.70(10)	3263.1(4)	3290.6(6)	3870.2(3)	2972.25(12)
Z	4	4	2	4	4
density (calcd), Mg/m^3	1.327	1.527	1.514	1.316	1.311
absorp coeff,mm^{-1}	0.517	3.386	3.357	0.453	0.568
cryst size, mm^3	0.20 × 0.20 × 0.15	0.55 × 0.50 × 0.45	0.20 × 0.15 × 0.15	0.27 × 0.25 × 0.17	0.25 × 0.20 × 0.15
reflns collected	14 977	32 344	44 214	38 826	11 688
indep reflns	7603	7489	13 182	8859	6802
data/restraints/params	7603/0/370	7489/0/370	13 182/0/740	8859/0/442	6802/0/326
final R indices [$I > 2\sigma(I)$]	R1 = 0.0358, wR2 = 0.0897	R1 = 0.0402, wR2 = 0.1048	R1 = 0.0199, wR2 = 0.0419	R1 = 0.0505, wR2 = 0.1079	R1 = 0.0335, wR2 = 0.0836
R indices (all data)	R1 = 0.0598, wR2 = 0.1103	R1 = 0.0443, wR2 = 0.1080	R1 = 0.0410, wR2 = 0.0443	R1 = 0.0625, wR2 = 0.1151	R1 = 0.0512, wR2 = 0.0954
goodness-of-fit on F^2	1.025	1.041	0.881	1.057	1.045
largest diff peak, e Å^{-3}	0.367 and −0.455	4.181 and −2.495	0.592 and −0.516	0.557 and −0.570	0.414 and −0.518

Table 2. Selected Bond Distances (Å) and Angles (deg) for Newly Prepared Metallocene Complexes *anti*-3a, *anti*-4a, *syn*-4a, *syn*-3b, 3e, and Reference Systems

	anti-3a	*anti*-4a	*syn*-4a	*syn*-3b	3e	I-Me$_2$[a]	I-Ph$_2$[b]	III[c]
M−Cl	2.4136(7)	2.3852(10)	2.3780(8)	2.4083(8)	2.4078(6)	2.8020(6)	2.4227(10)	2.412(3)
	2.4263(7)	2.3973(10)	2.4012(9)	2.4276(7)	2.4336(6)	2.639(1)[d]	2.4283(10)	2.421(3)
M−C(1)	2.436(2)	2.431(4)	2.420(3)	2.450(2)	2.4388(19)	2.427(3)	2.442(4)	2.447(9)
M−C(2)	2.463(2)	2.448(4)	2.453(2)	2.492(3)	2.475(2)	2.464(3)	2.492(3)	2.488(11)
M−C(3)	2.601(2)	2.581(4)	2.588(3)	2.620(3)	2.616(2)	2.611(4)	2.630(4)	2.533(11)
M−C(4)	2.549(2)	2.518(4)	2.541(3)	2.539(3)	2.549(2)	2.549(4)	2.547(4)	
M−C(5)	2.481(2)	2.462(4)	2.465(3)	2.453(3)	2.465(2)	2.461(4)	2.457(4)	
M−Cp$_{Cent}$	2.196(2)	2.175(4)	2.182(3)	2.203(3)	2.200(2)		2.204(4)	
M−C(9)	2.407(2)	2.398(4)	2.401(3)	2.413(4)	2.423(2)	2.432(4)	2.426(3)	2.401(9)
M−C(10)	2.505(2)	2.484(4)	2.517(3)	2.503(3)	2.510(2)	2.512(4)	2.497(4)	2.554(9)
M−C(11)	2.677(2)	2.650(4)	2.681(3)	2.655(3)	2.654(2)	2.653(4)	2.666(4)	2.659(8)
M−C(12)	2.721(2)	2.706(4)	2.669(3)	2.679(3)	2.671(2)	2.688(4)	2.712(4)	
M−C(13)	2.576(2)	2.563(4)	2.532(3)	2.552(3)	2.565(2)	2.611(4)	2.588(4)	
M−Flu$_{Cent}$	2.271(2)	2.253(4)	2.250(3)	2.253(3)	2.255(2)		2.269(4)	
Cp$_{Cent}$−M−Flu$_{Cent}$	118.29(16)	118.7(3)	119.6(2)	116.7(2)	118.08(11)	118.5(3)	118.03(4)	117.15
C(1)−C(6)−C(9)	101.28(19)	101.7(3)	101.8(2)	98.7(2)	102.21(16)	100.2(3)	98.60(3)	101.6(7)
H(7)−C(6)−C(8)	107.7(2)	107.85(4)	106.5(2)	106.3(2)	109.2(2)[e,f]	105.3(3)[f]	104.00(4)[f]	

[a] Data from ref 1b. [b] Data from ref 3. [c] Data from ref 5. [d] The crystal structure is for a mixed chloro-iodo-zirconocene complex, and the Zr−Cl bond distances must be therefore considered with caution. [e] In the complex bearing a methylene-bridged ligand, the corresponding angle is H−C(6)−H. [f] In the complex bearing a R$_2$C-bridged ligand (where R = Me or Ph), the respective angle is C−C(6)−C.

in DSC (entry 8); these data suggest the participation of two different active species.[18,19] Although we cannot rationalize at that time this strikingly different behavior between the two diastereomeric precursors, this is, to our knowledge, a quite unique observation for *ansa*-metallocene complexes.

No polymerization activity was found for zirconocene complex **3b**, which bears a cumyl group in the Cp ring (entry 9). A similar inactivity was observed in the case of {Ph$_2$C-(3,6-*t*Bu$_2$Flu)(3-cumyl-5-Me-C$_5$H$_2$)}ZrCl$_2$/MAO in our previous study.[3] In both cases, it is assumed that a similar deactivation pathway operates, which involves coordination of the phenyl ring of the cumyl group onto the cationic metal center and subsequent C−H activation, yielding an inactive species.[3]

The methylene-bridged *ansa*-zirconocene complex **3e** generated a catalytic system with an activity (2320 kg PP·mol^{-1}·h^{-1}, entry 10) comparable to that of the reference systems **I-Me$_2$** and **I-Ph$_2$**, but ca. 1 order of magnitude lower than that based on **3a**. The PP produced with this system had similar molecular weights and polydispersities to the other three aforementioned catalysts, yet with a somewhat higher isotacticity ([*m*]^4 = 96.9%) as revealed by ^{13}C NMR spectroscopy and

(18) Propylene polymerization promoted by discrete but multisite (pyridylamide)hafnium post-metallocenes was recently reported; see: Busico, V.; Cipullo, R.; Pallecchia, R.; Rongo, L.; Talarico, G.; Macchioni, A.; Zuccaccia, C.; Froese, R. D. J.; Hustad, P. D. *Macromolecules* **2009**, *42*, 4369.

(19) Activation of metallocenes with commercial MAO is known to generate complex mixtures of species. For instance, activation of Cp*$_2$ZrMe$_2$ with MAO containing 30 mol % of AlMe$_3$ leads to mixtures of at least four different species, namely, Cp*$_2$Zr(Me)Me→[AlMe$_3$−(MAO)], [Cp*$_2$Zr(Me)(*μ*-Me)(Me)ZrCp$_2$]$^+$[Me(MAO)]$^-$, [Cp*$_2$Zr-(*μ*-Me)$_2$AlMe$_2$]$^+$[Me(MAO)]$^-$, and [Cp*$_2$Zr(Me)]$^+$←[Me−(MAO, AlMe$_3$)]$^-$; see: (a) Babushkin, D. E.; Semikolenova, N. V.; Zakharov, V. A.; Tasli, E. *Macromol. Chem. Phys.* **2000**, *201*, 558. (b) Merle, P. G.; Cheron, V.; Hagen, H.; Lutz, M.; Spek, A. L.; Deelman, B.-J.; Van Koten, G. *Organometallics* **2005**, *24*, 1620. The use of diastereomeric metallocenes may lead obviously to even more complex mixtures, with a distinct behavior for each diastereomeric precursor.

Table 3. Isoselective Propylene Polymerization[a]

entry	precatalyst	precatalyst (μmol)	MAO (equiv)	T_{polym} (°C)[b]	m_{iPP} (g)	product. (g/g of precatalyst)	activity (kg·mol^{-1}·h^{-1})	T_m (°C)[c]	M_w ($\times 10^3$)[d]	M_w/M_n[d]	[*m*]^4 (%)[e]	1,2-insert. (%)[e]
1	**I-Me$_2$**	11	5000	60 (61)	1.39	1390	1710	152	166	2.4	95.2	> 99.9
2	**I-Ph$_2$**	9	5000	60 (61)	2.42	2420	3580	152	175	2.3	94.0	> 99.9
3	***anti*-3a**	10	5000	40 (55)	13.50	13 500	18 000	155	230	2.3	94.8	> 99.9
4	***anti*-3a**	10	5000	60 (64)	10.55	10 550	14 000	153	171	2.6	95.8	> 99.9
5	***anti*-3a**	10	5000	80 (85)	12.76	12 760	16 920	133	50	2.1	82.2	99.8
6	***anti*/*syn*-3a** (40:60)	9	5000	60 (70)	9.61	10 680	14 160	151	154	2.3	94.0	> 99.9
7	***anti*-4a**	200	1000	40	2.05	170	260	142	72	2.7	88.8	> 99.9
8	***syn*-4a**	200	1000	40	2.18	180	270	146, 153	239	6.6[f]	94.0	> 99.9
9	***syn*-3b**	200	1000	60	0	0	0					
10	**3e**	11	5000	60 (64)	1.98	1980	2320	154	180	2.4	96.9	> 99.9

[a] Polymerization conditions: 300 mL high-pressure glass reactor; solvent: toluene, 150 mL; *P*(propylene) = 5 bar; time = 30 min. See also reference15. [b] Data in brackets refer to the maximum temperature reached in the reactor. [c] Determined by DSC. [d] Determined by GPC. [e] Isotactic pentad content determined by ^{13}C NMR spectroscopy. [f] Bimodal distribution.

also the highest T_m value (154 °C) within the series of iPPs obtained in this study.

Conclusions

A new series of C_1-symmetric group 4 *ansa*-metallocene complexes incorporating monoaryl-substituted methylene-bridged {Flu-Cp} ligands was obtained through an inexpensive and effective synthetic approach. Neutral zirconium and hafnium complexes were produced, in most cases, as mixtures of diastereomers that depended on the nature of the ligand and metal. Crystallizations afforded pure diastereomers (***anti*-3a**, ***anti*-4a**, ***syn*-4a**, and ***syn*-3b**), which were independently authenticated and evaluated in propylene polymerization. Precursor ***anti*-3a**, when activated with MAO, appeared to be 1 order of magnitude more active than systems based on the reference precatalysts **I-Me$_2$** and **I-Ph$_2$**, while providing the same level of stereocontrol for the production of highly isotactic polypropylene. Such differences in the catalytic behavior are even more pronounced in the case of *ansa*-hafnocene precursors, where a multisite catalytic system is generated upon activation of ***syn*-4a** with MAO, while ***anti*-4a** leads to a single-site catalytic system.

The geometrical parameters of the molecules within this series of *ansa*-metallocene precursors are very similar; hence, the reason for the enhanced catalytic activity in complexes featuring a Ph(H)C bridge, as compared to CH_2- and CPh_2-bridged analogues, is not obvious. At this time, we can only hypothesize that the activation step of the propylene polymerization reaction mediated by ***anti*-3a**/MAO may produce active species dissimilar in nature from those derived from **I-Me$_2$** or **I-Ph$_2$**.[20] Such a phenomenon may also account for the strikingly different catalytic behavior observed between the diastereomeric *ansa*-hafnocene complexes ***syn*-** and ***anti*-4a**. Investigations aimed at clarifying the nature of the active species generated from Ph(H)C-bridged *ansa*-metallocene precatalysts as well as other structural modifications of this class of metallocene compounds to further improve on catalytic performance and control over iPP properties are underway and will be reported in due course.

(20) For instance, the stoichiometric reaction between Me(H)Si-bridged metallocenes {Me(H)Si-(η^5-C$_5$Me$_4$)(η^1-N*t*Bu)}TiMe$_2$ and {Me(H)Si-(η^5-indenyl)$_2$}ZrMe$_2$ and 2 equiv of [Ph$_3$C][B(C$_6$F$_5$)$_4$] resulted in simultaneous hydride and methide abstraction, to afford silylium-metallocenium heterodicationic complexes. The latter species, being highly electrophilic, appeared to be at least 2 times more active in propylene polymerization than the corresponding metallocenium monocations; see: Zhang, Y.; Chen, E. Y.-X. *J. Organomet. Chem.* **2010**, *695*, 1464.

Experimental Section

General Considerations. All manipulations (except polymerizations) were performed under a purified argon atmosphere using standard Schlenk techniques or in a glovebox. Solvents were distilled from Na/benzophenone (THF, Et$_2$O) and Na/K alloy (toluene, pentane) under nitrogen, degassed thoroughly, and stored under nitrogen prior to use. Deuterated solvents (benzene-d_6, toluene-d_8, THF-d_8; > 99.5% D, Deutero GmbH and Euroisotop) were vacuum-transferred from Na/K alloy into storage tubes. $CDCl_3$, CD_2Cl_2, and $C_2D_2Cl_4$ were kept over CaH_2 and vacuum-transferred before use. The ligand precursor 3,6-di-*tert*-butylfluorene was generously provided by Total Petrochemicals. The precursors 3,6,6′-trimethylfulvene, 1-*tert*-butyl-3-methylcyclopentadiene (mixture of isomers), and 1-methyl-3-*tert*-butylcyclopentadienyllithium were prepared according to reported protocols[21] and characterized by ^{1}H NMR spectroscopy. 1-Cumyl-3-methylcyclopentadiene was synthesized as previously described.[3] The reference metallocene complex {Me$_2$C-(3,6-*t*Bu$_2$Flu)(3-*t*Bu-5-MeC$_5$H$_2$)}ZrCl$_2$ (**I-Me$_2$**) was synthesized as described in the patent literature.[21] MAO (30 wt % solution in toluene, Albermarle; contains ca. 10 wt % of free AlMe$_3$) was used as received. Other starting materials were purchased from Acros, Strem, and Aldrich and used as received.

NMR spectra were recorded on Bruker AC-200, AC-300, AM-400, and AM-500 spectrometers in Teflon-valved NMR tubes at 25 °C, unless otherwise indicated. ^{1}H and ^{13}C chemical shifts are reported in ppm vs SiMe$_4$ or determined by reference to the residual solvent peaks. ^{19}F chemical shifts were determined by external reference to an aqueous solution of $NaBF_4$. Assignments of resonances for organometallic complexes were made from 2D ^{1}H−^{13}C HMQC and HMBC NMR experiments. Coupling constants are given in hertz. Elemental analyses (C, H, N) were performed using a Flash EA1112 CHNS Thermo Electron apparatus and are the average of two independent determinations. FAB-HRMS spectra were recorded on a high-resolution MS/MS Micromass ZABSpecTOF spectrometer. DSC measurements were performed on a SETARAM Instrumentation DSC 131 differential scanning calorimeter at heating rate of 10 °C/min; first and second runs were recorded after cooling to 30 °C; the reported melting temperatures correspond to the second run. GPC analyses of iPP samples were carried out in 1,2,4-trichlorobenzene at 135 °C at the Total Petrochemicals research center in Feluy (Belgium), using polystyrene standards for universal calibration. ^{13}C NMR analyses of iPP samples were run on a AM-500 Bruker spectrometer (Total Petrochemicals, Feluy, Belgium) as follows: solutions of ca. 200 mg of PP polymer in a trichlorobenzene/C$_6$D$_6$ mixture at 135 °C in 10 mm tubes, inverse gated experiment, pulse angle 90°, delay 11 s, acquisition time 1.25 s, number of scans 6000.

(21) Razavi, A. (Atofina Co.) *PCT Int. Appl.* WO00/49029, 1999.

6-Phenyl-2-methyl-4-*tert*-butylfulvene (1a). To a solution of 1-methyl-3-*tert*-butylcyclopentadiene (1.94 g, 14.24 mmol; mixture of isomers) in diethyl ether (50 mL) was added *n*-butyllithium (5.70 mL of a 2.50 M solution in hexane, 14.24 mmol) at 0 °C. The mixture was stirred for 2 h, and a solution of benzaldehyde (1.44 mL, 14.24 mmol) in diethyl ether (30 mL) was added dropwise. The reaction mixture turned orange. After 2 h, concentrated aqueous NH_4Cl (50 mL) was added slowly. This mixture was stirred overnight. The organic layer was separated and dried over $MgSO_4$, and the volatiles were removed *in vacuo*. The orange residue was recrystallized from methanol at −30 °C to give **1a** as a deep-red solid (1.00 g, 4.46 mmol, 31%). ^{1}H NMR ($CDCl_3$, 400 MHz, 25 °C): δ 7.57 (m, 2H, Ph), 7.40 (m, 3H, Ph), 7.01 (s, 1H, C*H*Ph), 6.24 (t, J = 1.7, 1H, C*H*), 6.14 (s, 1H, C*H*), 2.15 (s, 3H, CH_3), 1.19 (s, 9H, CCH_3). Anal. Calcd for $C_{17}H_{20}$: C, 91.01; H, 8.99. Found: C, 91.18; H, 9.33.

6-Mesityl-2-methyl-3-cumylfulvene (1b). To a 50 mL round-bottom flask containing 1-cumyl-3-methylcyclopentadiene (1.00 g, 5.05 mmol; mixture of isomers) was added 2,4,6-trimethylbenzaldehyde (0.76 g, 5.23 mmol) and absolute ethanol (20 mL). Once the solids had dissolved, NaOMe (0.55 g, 10.18 mmol) was added and the mixture was stirred for 7 days. The yellow precipitate was filtered, washed with methanol (2 × 5 mL), and dried *in vacuo* to yield **1b** as a yellow solid (1.10 g, 3.35 mmol, 66%). ^{1}H NMR ($CDCl_3$, 200 MHz, 25 °C): δ 7.40−7.10 (m, 5H, Ph), 6.96 (m, 3H, Ph), 5.86 (s, 1H, C*H*), 5.72 (s, 1H, C*H*), 2.35 (s, 3H, CH_3), 2.27 (s, 6H, CH_3), 2.11 (s, 3H, CH_3), 1.49 (s, 6H, CH_3). Anal. Calcd for $C_{25}H_{28}$: C, 91.41; H, 8.59. Found: C, 91.99; H, 9.02.

6-(3,5-Bis(trifluoromethyl)phenyl)-3-*tert*-butyl-5-methylfulvene (1c). A protocol similar to that described above for **1a** was used, starting from 1-methyl-3-*tert*-butylcyclopentadiene (2.81 g, 20.63 mmol; mixture of isomers), *n*-butyllithium (8.20 mL of a 2.50 M solution in hexane, 20.63 mmol), and 3,5-bis(trifluoromethyl)-benzaldehyde (5.00 g, 20.65 mmol). Workup afforded **1c** as a red solid (2.60 g, 7.22 mmol, 35%). ^{1}H NMR ($CDCl_3$, 300 MHz, 25 °C): δ 7.92 (s, 2H, Ph), 7.79 (s, 1H, Ph), 6.95 (s, 1H, C*H*Ph), 6.25 (t, J = 1.7, 1H, C*H*), 5.92 (s, 1H, C*H*), 2.11 (s, 3H, CH_3), 1.15 (s, 9H, CCH_3). ^{19}F NMR ($CDCl_3$, 282 MHz, 25 °C): δ −62.6. Anal. Calcd for $C_{19}H_{18}F_6$: C, 63.33; H, 5.03. Found: C, 63.67; H, 5.58.

6-Trifluoromethyl-6′-phenyl-2-methyl-3-*tert*-butylfulvene (1d). To a solution of 1-methyl-3-*tert*-butylcyclopentadiene (4.00 g, 29.36 mmol; mixture of isomers) in THF (50 mL) was added *n*-butyllithium (18.40 mL of a 1.60 M solution in hexane, 29.44 mmol) at 0 °C. The mixture was stirred for 2 h, and a solution of trifluoromethyl phenyl ketone (5.00 g, 28.71 mmol) in THF (20 mL) was added dropwise. After 2 h, HCl (50 mL of a 2 M aqueous solution) was added slowly. This mixture was stirred overnight. The organic layer was separated and dried over $MgSO_4$, and the volatiles were removed *in vacuo*. The orange residue was redissolved in pentane, and the resulting solution was passed through a short silica column and concentrated to give after crystallization at −30 °C **1d** as an orange solid (2.10 g, 7.18 mmol, 25%). ^{1}H NMR ($CDCl_3$, 200 MHz, 25 °C): δ 7.46−7.25 (m, 5H, Ph), 6.22 (m, 1H, =C*H*), 6.14 (m, 1H, C*H*), 1.25 (s, 3H, CH_3), 1.19 (s, 9H, CCH_3). ^{19}F NMR ($CDCl_3$, 188 MHz, 25 °C): δ −56.3. Anal. Calcd for $C_{18}H_{19}F_3$: C, 73.95; H, 6.55. Found: C, 73.84; H, 6.87.

6-Dimethylamino-2-methyl-4-*tert*-butylfulvene (1e). DMF (5.40 g, 73.80 mmol) and dimethylsulfate (9.21 g, 73.80 mmol) were stirred overnight at room temperature. To this mixture was added a solution of 1-methyl-3-*tert*-butylcyclopentadienyl potassium (prepared from the corresponding cyclopentadiene (10.0 g, 73.42 mmol; mixture of isomers) and KH (3.20 g, 80.00 mmol)). The mixture was stirred for 4 h at room temperature, and the volatiles were then removed under reduced pressure. The oily residue was distilled (ca. 120−140 °C/10^{-2} Torr) to give **1e** (3.20 g, 16.73 mmol, 23%) as an orange-yellow oil, which crystallized at room temperature. *This compound rapidly decomposes in the presence of moisture, and it is recommended that it be stored and handled in the glovebox.* ^{1}H NMR ($CDCl_3$, 400 MHz, 25 °C): δ 6.96 (s, 1H, C*H*N), 6.18 (s, 1H, C*H*), 6.12 (s, 1H, C*H*), 3.22 (s, 6H, NCH_3), 2.24 (s, 3H, CH_3), 1.27 (s, 9H, CCH_3). Anal. Calcd for $C_{13}H_{21}N$: C, 81.61; H, 11.06. Found: C, 82.04; H, 11.79.

3,6-Di-*tert*-butyl-9-[(3-*tert*-butyl-5-methylcyclopenta-1,4-dienyl)-phenylethyl]-9*H*-fluorene (2a). To a solution of **1a** (1.75 g, 7.80 mmol) in THF (20 mL) was added at room temperature a solution of 3,6-di-*tert*-butylfluorenyllithium (30 mL) prepared from 3,6-di-*tert*-butylfluorene (1.95 g, 7.00 mmol) and *n*-butyllithium (2.80 mL of a 2.50 M solution in hexane, 7.00 mmol). The mixture was stirred for 4 h at room temperature, quenched with saturated aqueous NH_4Cl (50 mL), and diluted with diethyl ether (50 mL). The organic layer was separated, washed with water (2 × 200 mL), and dried over $CaCl_2$. The volatiles were removed *in vacuo*. The residue was dissolved in hot methanol (50 mL). The solution was cooled to −30 °C, and a white precipitate formed. The precipitate was filtered, washed with cold methanol (−30 °C), and dried *in vacuo* overnight to give **2a** as a white powder (2.30 g, 4.57 mmol, 65%). ^{1}H NMR ($CDCl_3$, 300 MHz, 25 °C): δ 7.70 (m, 2H, Flu), 7.35 (m, 5H, Ph), 7.08 (dd, J = 2.5, J = 10.8, 1H, Flu), 6.95 (dd, J = 2.5, J = 10.8, 1H, Flu), 6.83 (d, J = 10.8, 1H, Flu), 6.29 (m, 2H, Cp), 4.48 (d, 1H, J = 10.6, C*H*Ph), 3.68 (d, 1H, ^3J = 10.6, 9-Flu), 2.79 (s, 2H, CH_2, Cp), 1.60 (s, 3H, CH_3), 1.37 (s, 9H, CCH_3-Flu), 1.33 (s, 9H, CCH_3-Flu), 1.14 (s, 9H, CCH_3-Cp). Anal. Calcd for $C_{38}H_{46}$: C, 90.78; H, 9.22. Found: C, 90.69; H, 9.11.

3,6-Di-*tert*-butyl-9-{mesityl[2-methyl-4-(1-methyl-1-phenylethyl)-cyclopenta-1,3-dien-1-yl]methyl}-9*H*-fluorene (2b). To a solution of **1b** (1.10 g, 3.35 mmol) in diethyl ether (20 mL) was added at room temperature 30 mL of a solution of 3,6-di-*tert*-butylfluorenyllithium prepared from 3,6-di-*tert*-butylfluorene (0.93 g, 3.34 mmol) and *n*-butyllithium (1.34 mL of a 2.50 M solution in hexane, 3.34 mmol). The mixture was refluxed for 5 days and quenched with saturated aqueous NH_4Cl (50 mL). The organic layer was separated, washed with water (2 × 200 mL), and dried over $MgSO_4$. The volatiles were removed *in vacuo*, and the residue was recrystallized from hot methanol to give white crystals of **2b** (1.35 g, 2.22 mmol, 67%). ^{1}H NMR ($CDCl_3$, 200 MHz, 25 °C): δ 7.80 (m, 2H), 7.50−7.18 (m, 7H), 6.96 (dd, J = 1.6, 1H), 6.85 (m, 3H), 6.14 (d, J = 8.0, 1H), 4.78 (d, J = 10.4, 1H), 4.10 (d, J = 10.4, 1H), 2.74 (s, 2H, CH_2, Cp), 2.34 (s, 3H, CH_3), 2.13 (br s, 6H, CH_3-Mes), 1.65 (s, 3H, CCH_3CH$_3$Ph), 1.64 (s, 3H, CCH$_3$CH_3Ph), 1.49 (s, 3H, CH_3-Mes), 1.48 (s, 9H, CCH_3-Flu), 1.40 (s, 9H, CCH_3-Flu). Anal. Calcd for $C_{38}H_{46}$: C, 90.78; H, 9.22. Found: C, 90.69; H, 9.11.

9-[[3,5-Bis(trifluoromethyl)phenyl](4-*tert*-butyl-2-methylcyclopenta-1,4-dien-1-yl)methyl]-3,6-di-*tert*-butyl-9*H*-fluorene (2c). Using a protocol similar to that described above for **2a**, compound **2c** was obtained from **1c** (2.60 g, 7.21 mmol) and 3,6-di-*tert*-butylfluorenyllithium (prepared from 3,6-di-*tert*-butylfluorene (2.00 g, 7.20 mmol) and *n*-butyllithium (2.88 mL of a 2.50 M solution in hexane, 7.20 mmol)). A similar workup afforded **2c** (0.200 g, 0.31 mmol, 4%) as an off-white solid. ^{1}H NMR ($CDCl_3$, 300 MHz, 25 °C): δ 7.70 (m, 3H, Ph), 7.20−6.30 (m, 6H, Flu), 6.20 (s, 1H, C*H*), 5.91 (s, 1H, C*H*), 4.48 (m, 1H, C*H*Ph), 3.95 (m, 1H, 9-Flu), 3.19−2.73 (m, 2H, CH_2), 1.59−1.52 (s, 3H, CH_3), 1.36−1.33 (s, 18H, CCH_3-Flu), 1.16−1.14 (s, 9H, CCH_3-Flu). ^{19}F NMR ($CDCl_3$, 282 MHz, 25 °C): δ −62.41, −62.45. Anal. Calcd for $C_{40}H_{44}F_6$: C, 75.21; H, 6.94. Found: C, 75.84; H, 7.01.

3,6-Di-*tert*-butyl-9-[1-(5-*tert*-butyl-2-methylcyclopenta-1,4-dien-1-yl)-2,2,2-trifluoro-1-phenylethyl]-9*H*-fluorene (2d). Using a protocol similar to that described above for **2a**, compound **2d** was obtained from **1d** (2.10 g, 7.18 mmol) and 3,6-di-*tert*-butylfluorenyllithium (prepared from 3,6-di-*tert*-butylfluorene (1.90 g, 6.82 mmol) and *n*-butyllithium (2.73 mL of a 2.50 M solution in hexane, 6.82 mmol)). A similar workup gave **2d** (2.00 g, 3.50 mmol, 49%) as a yellowish solid. ^{1}H NMR ($CDCl_3$, 200 MHz, 25 °C): δ 7.85−7.65 (m, 3H), 7.60−7.30 (m, 4H), 7.28−6.90 (m, 5H), 6.14 (s, 1H, C*H*), 4.95 (s, 1H, 9-Flu) 3.09 (br s, 2H, CH_2),

1.45 (s, 3H, CH_3), 1.40 (s, 18H, CCH_3-Flu), 1.16 (s, 9H, CCH_3-Flu). ^{19}F NMR ($CDCl_3$, 188 MHz, 25 °C): δ −59.1. Anal. Calcd for $C_{39}H_{45}F_3$: C, 82.07; H, 7.95. Found: C, 82.13; H, 7.63.

3,6-Di-*tert*-butyl-9-[(3-*tert*-butyl-5-methylcyclopenta-1,4-dien-1-yl)methyl]-9*H*-fluorene (2e). To a solution of **1e** (3.20 g, 16.70 mmol) in THF (50 mL) was added at room temperature a solution of 3,6-di-*tert*-butylfluorenyllithium (50 mL) prepared from 3,6-di-*tert*-butylfluorene (4.65 g, 16.7 mmol) and *n*-butyllithium (6.70 mL of a 2.50 M solution in hexane, 16.7 mmol). The mixture was stirred for 12 h at room temperature. $LiAlH_4$ (1.17 g, 30.8 mmol) was added, and the resulting mixture was refluxed for another 12 h. The mixture was carefully quenched with saturated aqueous NH_4Cl (50 mL) and diluted with diethyl ether (100 mL). The organic layer was separated, washed with water (2 × 200 mL), and dried over $CaCl_2$. The volatiles were removed *in vacuo*, and the crude product was purified by flash chromatography (thin pad of silica gel, pentane as eluent) to give **2e** as a yellow solid (4.27 g, 10.0 mmol, 60%). ^{1}H NMR ($CDCl_3$, 300 MHz, 25 °C): δ 7.78 (s, 2H, Flu), 7.40−7.10 (m, 4H, Flu), 6.18 (s, 1H, CH), 5.97 (s, 1H, CH), 4.00 (m, 1H, 9-Flu), 3.00 (m, 2H, CH_2), 2.70 (m, 2H, CH_2), 1.73, 1.66 (s, 3H, CH_3), 1.42 (s, 18H, CCH_3-Flu), 1.21 (s, 9H, CCH_3-Flu). Anal. Calcd for $C_{32}H_{42}$: C, 90.08; H, 9.92. Found: C, 90.50; H, 9.99.

{Ph(H)C-(3,6-*t*Bu$_2$Flu)(3-*t*Bu-5-Me-Cp)}ZrCl$_2$ (3a). To a solution of **2a** (1.03 g, 2.04 mmol) in diethyl ether (40 mL) was added *n*-butyllithium (1.67 mL of a 2.50 M solution in hexane, 4.08 mmol) at 0 °C with stirring. After 12 h, anhydrous $ZrCl_4$ (0.48 g, 2.04 mmol) was added to the sample in the glovebox. The resulting pink reaction mixture was stirred at room temperature overnight. Then volatiles were evaporated *in vacuo*, and hexane (ca. 40 mL) was vacuum-transferred under reduced pressure. The mixture was filtered, and the solvent was removed from the filtrate to give **3a** as a pink powder (1.18 g, 1.78 mmol, 88%); this material contained 90% of the *anti* isomer, as determined by ^{1}H NMR spectroscopy. The product was recrystallized from hexane (20 mL) at room temperature to yield pure *anti*-**3a** isomer (0.53 g, 8.80 mmol, 40% yield). Crystals suitable for X-ray diffraction studies were obtained by slow concentration of a CH_2Cl_2/hexane (1:9 v/v) solution. ^{1}H NMR (CD_2Cl_2, 300 MHz, 25 °C): δ 8.03 (m, 2H, Flu), 7.78 (d, J = 7.8, 2H), 7.58 (d, J = 9.1, 1H), 7.48 (m, 2H), 7.43 (m, 2H), 7.08 (dd, J = 1.8, J = 9.0, 1H, Flu), 6.57 (d, J = 9.0, 1H, Flu), 6.50 (s, 1H, CHPh), 6.12 (d, 1H, J = 2.6, Cp), 5.57 (d, 1H, J = 2.6, Cp), 2.21 (s, 3H, CH_3), 1.45 (s, 9H, CCH_3-Flu), 1.38 (s, 9H, CCH_3-Flu), 1.05 (s, 9H, CCH_3-Cp). ^{13}C NMR (CD_2Cl_2, 75 MHz, 25 °C): δ 150.2, 150.0, 147.1, 140.1, 129.2, 128.9, 128.6, 128.4, 128.2, 127.6, 126.7, 125.9, 125.3, 124.8, 122.8, 122.5, 121.5, 120.0, 119.5, 119.3, 116.9, 103.2, 100.9, 74.6 (9-Flu), 40.2 (*C*CH$_3$), 35.5 (*C*CH$_3$), 35.4 (*C*CH$_3$), 33.2 (C*C*H$_3$), 32.0 (C*C*H$_3$), 29.7 (C*C*H$_3$), 15.8 (*C*H$_3$). Anal. Calcd for $C_{38}H_{44}Cl_2Zr$: C, 68.85; H, 6.69. Found: C, 69.01; H, 6.78.

{Ph(H)C-(3,6-*t*Bu$_2$Flu)(3-*t*Bu-5-Me-Cp)}HfCl$_2$ (4a). Using a procedure similar to that described above for **3a**, crude **4a** was obtained from **2a** (1.11 g, 2.21 mmol), *n*-butyllithium (1.76 mL of a 2.50 M solution in hexane, 4.08 mmol), and anhydrous $HfCl_4$ (0.71 g, 2.21 mmol) in Et_2O (40 mL). The orange solid obtained after workup contained ca. 70% of the *anti* isomer, as estimated by ^{1}H NMR spectroscopy. Pure *anti*-**4a** was obtained by recrystallization from hexane (0.91 g, 1.21 mmol, 55%). ^{1}H NMR (CD_2Cl_2, 300 MHz, 25 °C): δ 8.07 (m, 2H, Flu), 7.81 (d, J = 8.3, 2H), 7.65 (d, J = 9.2, 1H), 7.60−7.43 (m, 3H), 7.42 (dd, J = 1.7, J = 9.0, 1H), 7.11 (dd, J = 1.7, J = 9.0, 1H, Flu), 6.68 (d, J = 9.2, 1H, Flu), 6.57 (s, 1H, PhHC), 6.10 (d, 1H, J = 2.6, Cp), 5.57 (d, 1H, J = 2.6, Cp), 2.36 (s, 3H, CH_3), 1.50 (s, 9H, CCH_3-Flu), 1.44 (s, 9H, CCH_3-Flu), 1.11 (s, 9H, CCH_3-Cp). ^{13}C NMR (CD_2Cl_2, 75 MHz, 25 °C): δ 149.1, 149.0, 145.3, 140.0, 128.8, 128.1, 127.7, 127.2, 126.1, 123.9, 122.9, 122.4, 122.1, 122.0, 119.5, 119.3, 118.9, 117.8, 115.5, 105.7, 98.1, 74.1 (9-Flu), 39.7 (*C*CH$_3$), 35.1 (*C*CH$_3$), 34.9 (*C*CH$_3$), 32.8 (*C*CH$_3$), 31.6 (C*C*H$_3$), 31.5, 29.3 (C*C*H$_3$), 15.2 (*C*H$_3$). Anal. Calcd for $C_{38}H_{44}Cl_2Hf$: C, 60.84; H, 5.91. Found: C, 60.92; H, 5.90.

Subsequent concentration under reduced pressure of the resulting mother liquor gave pure ***syn*-4a** (0.30 g, 0.40 mmol, 18%). ^{1}H NMR (CD_2Cl_2, 300 MHz, 25 °C): δ 8.08 (s, 1H), 8.04 (s, 1H), 7.88 (d, J = 8.4 Hz, 2H), 7.55 (m, 2H), 7.52−7.43 (m, 3H), 7.12 (dd, J = 1.7 Hz, J = 9.8 Hz, 1H), 7.04 (d, J = 9.2 Hz, 1H), 6.55 (s, 1H, PhHC), 6.05 (d, 1H, ^4J = 2.6 Hz, Cp), 5.52 (d, 1H, ^4J = 2.6 Hz, Cp), 1.98 (s, 3H, CH_3), 1.51 (s, 9H, CCH_3-Flu), 1.44 (s, 9H, CCH_3-Flu), 1.15 (s, 9H, CCH_3-Cp). ^{13}C NMR (CD_2Cl_2, 75 MHz, 25 °C): (three signals from quaternary carbons in the aromatic region were not observed) 149.5, 148.9, 143.7, 128.5, 128.3, 127.4, 127.3, 126.4, 125.3, 121.9, 120.5, 120.3, 120.2, 119.6, 119.4, 119.2, 119.1, 103.6, 101.6, 72.2 (9-Flu), 43.0 (*C*CH$_3$), 35.0 (*C*CH$_3$), 34.9 (*C*CH$_3$), 32.5 (*C*CH$_3$), 31.6 (C*C*H$_3$), 29.5 (C*C*H$_3$), 28.3 (C*C*H$_3$), 17.8 (*C*H$_3$). Anal. Calcd for $C_{38}H_{44}Cl_2Hf$: C, 60.84; H, 5.91. Found: C, 61.05; H, 5.99.

{Mes(H)C-(3,6-*t*Bu$_2$Flu)(3-CMe$_2$Ph-5-Me-Cp)}ZrCl$_2$ (3b). Using a protocol similar to that described above for **3a**, compound **3b** was prepared from **2b** (1.35 g, 2.22 mmol) and $ZrCl_4$ (0.52 g, 2.23 mmol) and isolated as a pink solid (1.07 g, 1.40 mmol, 63%). ^{1}H NMR (CD_2Cl_2, 300 MHz, 25 °C): δ 8.14 (s, 1H), 8.06 (s, 1H), 7.51 (s, 2H), 7.30−6.98 (m, 8H), 6.95 (s, 1H), 6.50 (s, 1H, MesCH), 6.01(d, 1H, J = 3.1, Cp), 5.63 (d, 1H, J = 3.1, Cp), 2.56 (s, 3H, Me), 2.40 (s, 3H, CH_3), 2.15 (s, 3H, CH_3), 1.87 (s, 3H, CH_3), 1.74 (s, 3H, CH_3), 1.53 (s, 9H, CCH_3-Flu), 1.45 (s, 9H, CCH_3-Flu), 1.42 (s, 3H, CH_3). ^{13}C NMR (CD_2Cl_2, 75 MHz, 25 °C): δ 152.1, 150.2, 149.7, 142.1, 137.9, 137.7, 136.5, 131.4, 130.6, 130.5, 127.9, 127.1, 125.5, 125.4, 125.0, 122.9, 122.1, 121.8, 121.5, 120.1, 119.9, 119.4, 119.1, 105.2, 102.5, 76.5 (9-Flu), 41.3 (*C*CH$_3$), 35.2 (*C*CH$_3$), 35.0 (*C*CH$_3$), 31.7 (C*C*H$_3$), 27.1 (C*C*H$_3$), 25.8 (C*C*H$_3$), 22.9 (*C*H$_3$), 21.9 (*C*H$_3$), 20.4 (*C*H$_3$), 17.4 (*C*H$_3$). Anal. Calcd for $C_{46}H_{52}Cl_2Zr$: C, 72.03; H, 6.83. Found: C, 72.86; H, 7.07.

{H$_2$C-(3,6-*t*Bu$_2$Flu)(3-*t*Bu-5-Me-Cp)}ZrCl$_2$ (3e). Using a protocol similar to that described above for **3a**, compound **3e** was prepared from **2e** (1.67 g, 3.91 mmol) and $ZrCl_4$ (0.91 g, 3.90 mmol) and isolated as a pink solid (1.48 g, 2.52 mmol, 64%). Crystals suitable for X-ray diffraction studies were obtained by slow concentration of a CH_2Cl_2/hexane (3:7 v/v) solution. ^{1}H NMR (CD_2Cl_2, 300 MHz, 25 °C): δ 8.01 (s, 1H, Flu), 7.97 (s, 1H, Flu), 7.52 (s, 1H, Flu), 7.40 (m, 2H, Flu), 7.37 (m, 1H, Flu), 6.02 (d, 1H, J = 2.8, Cp), 5.52 (d, 1H, J = 2.8, Cp), 4.74 (m, 2H, CH_2), 2.16 (s, 3H, CH_3), 1.44 (s, 9H, CCH_3-Flu), 1.43 (s, 9H, CCH_3-Flu), 1.05 (s, 9H, CCH_3-Flu). ^{13}C NMR (CD_2Cl_2, 75 MHz, 25 °C): δ 150.1, 150.0, 146.4, 127.9, 127.6, 124.8, 124.1, 124.0, 123.3, 121.8, 120.7, 120.6, 120.2, 119.7, 118.2, 102.4, 97.0, 70.3 (9-Flu), 35.6 (*C*CH$_3$), 33.3 (*C*CH$_3$), 32.2 (*C*CH$_3$), 32.1 (C*C*H$_3$), 32.0 (C*C*H$_3$), 30.0 (C*C*H$_3$), 22.5 (*C*H$_2$), 16.1 (*C*H$_3$). Anal. Calcd for $C_{32}H_{40}Cl_2Zr$: C, 65.50; H, 6.87. Found: C, 66.01; H, 6.99.

Propylene Polymerization. Polymerization experiments were performed in a 300 mL high-pressure glass reactor equipped with a mechanical stirrer (Pelton turbine) and externally heated with a double mantle with a thermostated circulating water bath. The reactor was charged with toluene (80 to 150 mL) and MAO (1.5 mL of a 30 wt % solution in toluene), and propylene (5 bar, Air Liquide, 99.99%) was introduced. The reactor was thermally equilibrated at the desired temperature for 30 min. Propylene pressure was decreased to 1 bar, and a solution of the catalyst precursor in toluene (ca. 2 mL) was added by syringe. The propylene pressure was immediately increased to 5 bar (kept constant with a back regulator), and the solution was stirred for the desired time. The temperature inside the reactor was monitored using a thermocouple. The polymerization was stopped by venting the vessel and quenching with a 10 wt % solution of aqueous HCl in methanol (ca. 3 mL). The polymer was precipitated in methanol (ca. 200 mL), and 35 wt % aqueous HCl (ca. 1 mL) was added to dissolve possible catalyst residues. The polymer was collected by filtration, washed with methanol (ca. 200 mL), and dried under vacuum overnight.

Crystal Structure Determination of *anti*-3a, *syn*-3b, *anti*-4a, *syn*-4a, and 3e. Diffraction data were collected at 100(2) or

173(2) K using a Bruker APEX CCD diffractometer with graphite-monochromatized Mo Kα radiation ($\lambda = 0.71073$ Å). A combination of ω and ϕ scans was carried out to obtain a unique data set. The crystal structures were solved by direct methods; remaining atoms were located from difference Fourier synthesis followed by full-matrix least-squares refinement based on F^2 (programs SIR97 and SHELXL-97).[22] Many hydrogen atoms could be located from the Fourier difference analysis. Other hydrogen atoms were placed at calculated positions and forced to ride on the attached atom. The hydrogen atom positions were calculated but not refined. All non-hydrogen atoms were refined with anisotropic displacement parameters. Crystal data and details of data collection and structure refinement for the different compounds are given in Table 1. Note that in ***syn*-4a** the asymmetric unit is composed of two independent molecules, each with the corresponding enantiomer. Detailed crystallographic data (excluding structure factors) are available as Supporting Information, as cif files.

(22) (a) Sheldrick, G. M. *SHELXS-97, Program for the Determination of Crystal Structures*; University of Goettingen: Germany, 1997. (b) Sheldrick, G. M. *SHELXL-97, Program for the Refinement of Crystal Structures*; University of Goettingen: Germany, 1997. (c) Sheldrick, G. M. *Acta Crystallogr*. **2008**, *A64*, 112.

Acknowledgment. This work was financially supported by Total Petrochemicals (grant to E.K., J.A.G., N.M., and M.B.). J.F.C. thanks the Institut Universitaire de France for a Junior IUF fellowship (2005−2009). Dr. Loic Toupet (IPR) and S. Sinbandhit (CRMPO) are gratefully acknowledged for technical assistance with X-ray diffraction and NMR spectroscopy experiments, respectively.

Supporting Information Available: Representative ^{1}H NMR spectra of fulvenes, proligands, and metallocene complexes, ^{13}C NMR spectrum of an iPP, and crystallographic data for ***anti*-3a**, ***syn*-3b**, ***anti*-4a**, ***syn*-4a**, and **3e** as CIF files. This material is available free of charge via the Internet at http://pubs.acs.org.